Journal of Photochemistry and Photobiology A: Chemistry 208 (2009) 50–58

Contents lists available at ScienceDirect

Journal of Photochemistry and Photobiology A: Chemistry

journal homepage: www.elsevier.com/locate/jphotochem

On the mechanism of the photoinduced reduction of an adduct of ferricytochrome C with a poly(4-vinylpyridine) polymer containing –$Re^{I}(CO)_3$(3,4,7,8-tetramethyl-1,10-phenanthroline) pendants

Larisa L.B. Bracco [a], Fernando S. García Einschlag [a], Ezequiel Wolcan [a,*], Guillermo J. Ferraudi [b,*]

[a] Instituto de Investigaciones Fisicoquímicas Teóricas y Aplicadas (INIFTA, UNLP, CCT La Plata-CONICET), Diag. 113 y 64, Sucursal 4, C.C. 16, (B1900ZAA) La Plata, Argentina
[b] Department of Chemistry, Radiation Research Building, University of Notre Dame, Notre Dame, IN 46556-0579, USA

ARTICLE INFO

Article history:
Received 2 July 2009
Received in revised form 6 August 2009
Accepted 14 August 2009
Available online 20 August 2009

Keywords:
Cytochrome c
Rhenium
Polymers
Photoinduced
MLCT
TEA

ABSTRACT

Changes in the UV–vis absorption spectrum revealed the formation of adducts between the Re^{I} polymer and ferricytochrome C, Fe^{III}-Cyt c. Different morphologies for the Re^{I} polymer and the adducts formed between the Re^{I} polymer and Fe^{III}-Cyt c were observed by TEM. The reduction of the Re^{I} chromophores in the polymer, achieved by the reductive quenching of the MLCT excited state of the Re^{I} polymer by triethylamine (TEA) and/or by the reaction between e^{-}_{solv} and $\{[(vpy)_2vpyRe^{I}(CO)_3(tmphen)^{+}]\}_{n\sim200}$ in pulse radiolysis experiments, produces $-Re^{I}(CO)_3(tmphen)^{\bullet}$ and $-Re^{I}(CO)_3(tmphenH)^{\bullet+}$ as the main species. The reductive quenching of the MLCT of the Re^{I} polymer by TEA was followed by a rapid electron transfer from the $-Re^{I}(CO)_3(tmphen)^{\bullet}$ to the Fe^{III} center in the heme to produce ferrocytochrome C, Fe^{II}-Cyt c.

1. Introduction

Fe^{III}-Cyt c is a small protein, ~12 kDa, consisting of a single 104 amino acid peptide with a single heme group, Scheme 1. Because of its ubiquitous nature and sequence homology, Fe^{III}-Cyt c has been used as a model protein for molecular evolution [1–3,4a]. Fe^{III}-Cyt c is primarily known as an electron-carrying mitochondrial protein. The interconversion of Fe^{II}-Cyt c and Fe^{III}-Cyt c within the cell makes it an efficient biological electron carrier and it plays a vital role in cellular oxidations in both plants and animals. It is generally regarded as a universal catalyst for the respiratory process, forming an essential electron bridge between the substrates and oxygen. At a cellular level, its main function is to transport electrons from cytochrome c reductase to cytochrome c oxidase. Biological synthesis of Fe^{III}-Cyt c occurs in the intermembrane space of mitochondria. It involves heme ligation to apo Cyt c, which has a disordered structure in solution, and subsequent formation of the folded (native) Fe^{III}-Cyt c. On the other hand, the interaction of folded Fe^{III}-Cyt c with lipids resulted in a partial unfold of the native protein, and Fe^{III}-Cyt c was shown to exist in equilibrium between a soluble state and a membrane-bound state at physiological pH [4b]. Moreover, proteins that are partially or wholly disordered under physiological conditions can still perform important biological functions, such as molecular recognition, signaling, and regulation [4c]. Because the biological properties of proteins arise mainly from their native conformations, during the past 70 years considerably more attention has been focused on the native conformations than on the nonnative ones. In the past few years, however, there has been increasing interest in nonnative and denatured states of proteins since these less ordered states play important roles in at least three major phenomena: (1) Protein folding and stability, (2) Transport across membranes and (3) Proteolysis and protein turnover [4d,4e].

The goal of developing a detailed understanding of inter-protein electron transfer involves many complex problems since the reactions are dependent on many different factors such us electronic properties of the redox centers, the distance and pathway of electron transfer, the reorganization energy and the kinetics of complex formation and dissociation. The measurement of the rate of intramolecular electron transfer has been a particularly difficult problem since only a limited number of techniques are available which include stopped-flow spectroscopy, pulse radiolysis, flash photolysis [5a] and lately spectrolelectrochemistry combined with surface enhanced resonance Raman spectroscopy [5b].

Intramolecular electron transfer betweeen Fe^{III}-Cyt c and transition metal compounds has been investigated by attaching photoactive Ru complexes to the protein surface [5a,6–8]. In those studies, photoinduced electron transfer occurs between the

* Corresponding author.
E-mail addresses: ewolcan@inifta.unlp.edu.ar (E. Wolcan), ferraudi@hertz.rad.nd.edu (G.J. Ferraudi).

1010-6030/$ – see front matter © 2009 Elsevier B.V. All rights reserved.
doi:10.1016/j.jphotochem.2009.08.003

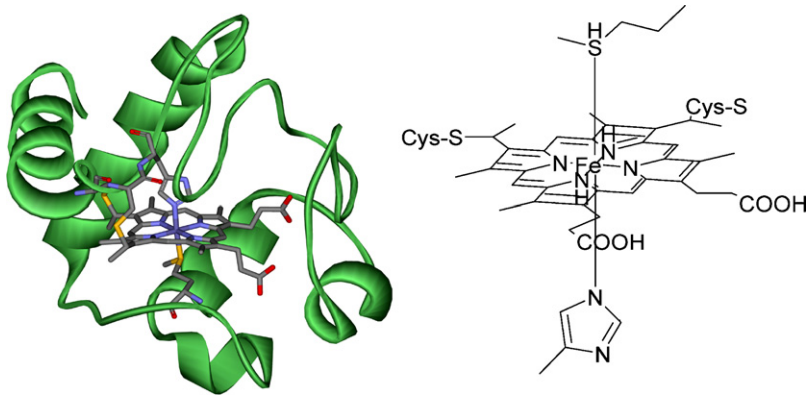

Scheme 1.

reducing excited state of $Ru^{II}(bpy)_2B_L^{2+}$ (B_L = bridging ligand) and the ferric heme group. However, as far as we know, there are no photoinduced electron transfer studies between Fe^{III}-Cyt c and Re^{I} complexes. $Re^{I}(CO)_3LL'$(L = diimine, L′ = halide or pyridine derivative) complexes are capable of acting as photocatalysts with the aid of a sacrificial reductant, eq. (1),

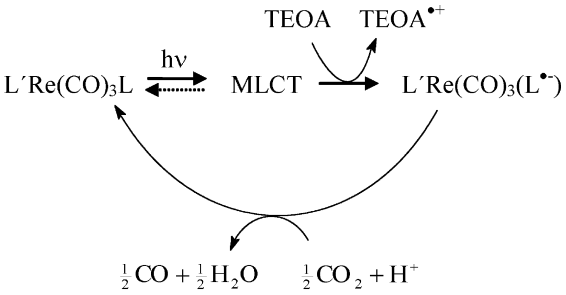

(L = polypyridine or phenanthroline derivative) (1)

It is known that reductive quenching of the lowest Re-to-bpy charge transfer excited state (MLCT) of the complex by triethanolamine (TEOA) generates a species, $[ClRe(CO)_3(bpy)]^{\bullet -}$, capable, for instance, of mediating the two-electron process of CO_2 reduction to CO [9].

On the other hand, numerous studies have dealt with thermal and photochemical reactions of inorganic polymers in the solid state and solution phase. Interest in their photochemical and photophysical properties is driven by their potential applications in catalysis and optical devices [10–21]. The photophysical properties in the solution phase of a Re^{I} containing polymer $[(vpy)_2vpyRe(CO)_3(tmphen)^+]\}_{n\sim200}$ (where tmphen = 3,4,7,8-tetramethyl-1,10 phenanthroline and vpy = 4-vinylpyridine, see Scheme 2), hereafter designated as ReP4VP, were investigated in previous work [22]. As poly(4-vinylpyridine) tends to interact with Fe^{III}-Cyt c by hydrogen bonding interactions [1], we decided to study the photocatalytic properties of the chromophores $Re(CO)_3(tmphen)^+$ in the reduction of Fe^{III}-Cyt c by using the polymer ReP4VP as a probe, since ReP4VP also interacts with Fe^{III}-Cyt c by the formation of adducts. In this paper we explore the photoinduced reduction of Fe^{III}-Cyt c by ReP4VP in CH_3CN/H_2O solutions, where the protein is denatured. The reductive quenching of the MLCT excited state of ReP4VP by triethylamine (TEA) produces -$Re^{I}(CO)_3(tmphen)^{\bullet}$ species in the polymer, which in the presence of Fe^{III}-Cyt c reduce the ferric iron of the heme portion of the protein to the ferrous state.

2. Materials and methods

2.1. Flash-photochemical procedures

Optical density changes occurring on a time scale longer than 10 ns were investigated with a flash photolysis apparatus described elsewhere [23–25]. In these experiments, 25 ns flashes of 351 nm (ca. 25 - 30 mJ/pulse) light were generated with a Lambda Physik SLL-200 excimer laser. The energy of the laser flash was attenuated to values equal to or lower than 20 mJ/pulse by absorbing some of the laser light by $Ni(ClO_4)_2$ solutions with appropriate optical transmittances, $T = I_t/I_0$, where I_0 and I_t are the intensities of the light arriving at and transmitted from the photolysis cell, respectively. The transmittance, $T = 10^{-A}$, was routinely calculated by using the spectrophotometrically measured absorbance, A, of the solution. A right angle configuration was used for the pump and the probe beams. Concentrations of the complexes were adjusted to provide homogeneous profiles of photogenerated intermediates over the probe beam optical path, l = 1 cm. To satisfy this optical condition, solutions were prepared with an absorbance equal to or less than 0.4 over the 0.2 cm optical path of the pump. All solutions used in the photochemical work were deaerated with streams of ultrahigh-purity N_2 before and during the irradiations.

2.2. Pulse radiolysis

Pulse radiolysis experiments were carried out with a model TB-8/16-1S electron linear accelerator. The instrument and computerized data collection for time-resolved UV–vis spectroscopy and reaction kinetics have been described elsewhere in the literature [26,27]. Thiocyanate dosimetry was carried out at the

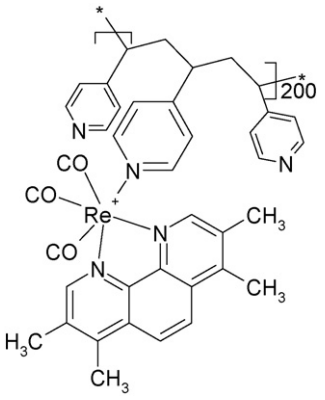

Scheme 2.

beginning of each experimental session. Details of the dosimetry have been reported elsewhere [26,28]. The procedure is based on the concentration of $(SCN)_2^{\bullet -}$ radicals generated by the electron pulse in an N_2O-saturated 10^{-2} M SCN^- solution. In the procedure, the calculations were made with $G = 6.13$ and an extinction coefficient $\varepsilon = 7.58 \times 10^3\ M^{-1}\ cm^{-1}$ at 472 nm [26,28] for the $(SCN)_2^{\bullet -}$ radicals. In general, the experiments were carried out with doses that in N_2-saturated aqueous solutions resulted in $(2.0 \pm 0.1) \times 10^{-6}$ M to $(6.0 \pm 0.3) \times 10^{-6}$ M concentrations of e^-_{aq}. In these experiments, solutions were deaerated with streams of the O_2-free N_2 or N_2O gasses. In order to irradiate a fresh sample with each pulse, an appropriate flow of the solution through the reaction cell was maintained during the experiment.

The radiolysis of CH_3OH and CH_3OH/H_2O mixtures with ionizing radiation has been reported elsewhere in the literature [29–31]. These studies have shown that pulse radiolysis can be used as a convenient source of e^-_{sol} and $C^{\bullet}H_2OH$ radicals according to eq. (2)

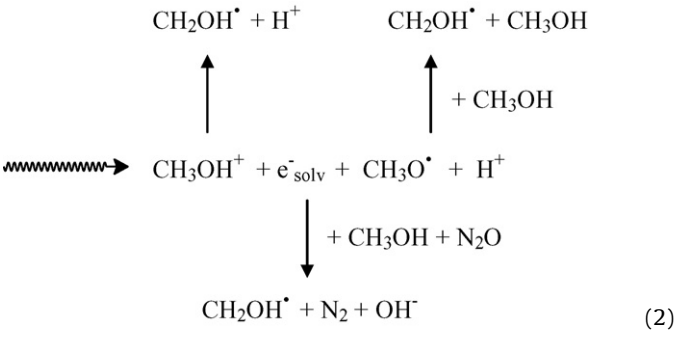

(2)

Since e^-_{sol} and $CH_2OH^{\bullet}$ have large reduction potentials, i.e., −2.8 V versus NHE for e^-_{sol} and −0.92 V versus NHE for $CH_2OH^{\bullet}$, they have been used for the reduction of coordination complexes and for the study of electron-transfer reactions. The yield of e^-_{sol} in CH_3OH ($G \approx 1.1$) is about a third of the G value in the radiolysis of H_2O ($G \approx 2.8$) [29]. In solutions where e^-_{sol} was scavenged with N_2O [31], the $CH_2OH^{\bullet}$ radical appears to be the predominant product (yield > 90%) of the reaction between CH_3OH and $O^{\bullet -}$.

2.3. TEM

Transmission electron micrographs were recorded on a Philips EM 301 electron microscope at an electron acceleration voltage of 60 kV.

2.4. General methods

UV–vis spectra were recorded on a Cary 3 spectrophotometer.

2.4.1. Materials

Reagent grade horse heart muscle Fe^{III}-Cyt c (M_w 12.384, anhydrous), Fe^{III}Cyt C, was purchased from Aldrich and used as received. ReP4VP was available from previous work [22].

2.4.2. Spectroscopic analysis

For the analysis of the time-resolved spectra we used a software for chemometric techniques designed in our laboratory [32a] in order to perform "multivariate self-modeling curve resolution" (MVCR) [32b]. These methods can be applied to bilinear spectroscopic-kinetic data from a chemical reaction to provide information about composition changes in an evolving system [32c]. In the present work we have chosen one of the most widely used algorithms, the alternating least-squares (ALS), which can help estimate concentration and spectral profiles simultaneously [32c,33]. ALS algorithms extract useful information from the experimental data matrix $\mathbf{A}(t \times w)$ by iterative application of regression analysis using the following matrix product:

$$\mathbf{A} = \mathbf{CS}^{\mathrm{T}} + \mathbf{E} \tag{3}$$

where $\mathbf{C}(t \times n)$ is the matrix of the kinetic profiles; $\mathbf{S}^{\mathrm{T}}(n \times w)$ is that containing the spectral profiles, and $\mathbf{E}(t \times w)$ represents the error matrix. The numbers $\boldsymbol{t}$, $\boldsymbol{n}$ and $\boldsymbol{w}$ denote the sampling times, absorbing species and recorded wavelengths, respectively. Resolving matrix $\mathbf{A}$ is no easy task [34a] since on the one hand, $\boldsymbol{n}$ is usually unknown [34b] and on the other hand, curve resolution methods cannot deliver a single solution because of the rotational and scale ambiguities. We applied Factor Analysis and Singular Value Decomposition to the experimental matrix for the estimation of $\boldsymbol{n}$. In order to reduce rotational ambiguities we used some chemically relevant constraints [34c] such as nonnegativity and unimodality for the kinetic profiles.

3. Results

The experimental observations communicated in the following sections showed that Fe^{III}Cyt c, in the denatured state, forms adducts with ReP4VP and that Fe^{III}Cyt c in the adducts is reduced to Fe^{II}-Cyt c in a photoprocess initiated by MLCT excited states of the polymer Re^I pendants.

3.1. Solution phase formation of adducts between ReP4VP and Fe^{III}-Cyt c

Changes in the UV–vis absorption spectrum revealed the formation of adducts between ReP4VP and Fe^{III}-Cyt c in acetonitrile/water (8:2, v:v). Indeed, the sum of the respective spectra of ReP4VP and Fe^{III}-Cyt c does not yield the spectrum of a solution containing both species. Moreover, the change in the shape of the difference spectra with the concentration of one compound or the other is indicative of a gradual displacement of the association equilibrium. Typical difference spectra, recorded with solutions containing 8.8×10^{-6} M Fe^{III}-Cyt c and various concentrations of ReP4VP ($[Re^I]$ between 8.8×10^{-6} M and 8.8×10^{-5} M), are shown in Fig. 1b. Fig. 1c shows the difference spectra recorded with solutions containing ReP4VP ($[Re^I] = 8.8 \times 10^{-6}$ M) and various concentrations of Fe^{III}Cyt C between 2.2×10^{-6} M and 8.8×10^{-6} M. To calculate the difference spectra in Fig. 1, the spectra of the two solutions containing ReP4VP and Fe^{III}-Cyt c, respectively, were subtracted from the spectrum of a solution having these species together and with the same concentrations of the two previous solutions (see Fig. 1a). The concentration dependences shown in Fig. 1b, c indicate that the interaction between Fe^{III}-Cyt c and ReP4VP reaches a maximum when the relationship between pendants and Fe^{III}-Cyt c is $[Re^I] \sim [Fe^{III}\text{-Cyt c}]$, i.e., the concentration of free pyridines is twice the concentration of Fe^{III}-Cyt c.

3.2. Morphologies of Fe^{III}-Cyt c, ReP4VP and the adduct

The morphologies of the polymer ReP4VP, Fe^{III}-Cyt c and the adduct formed between them were studied by transmission electron microscopy (TEM). When taking micrographs, the films were not stained with any chemicals, and the contrast of the image in the TEM micrographs can only originate from the rhenium and iron complexes incorporated to the polymers. Figs. 2 and 3 show the morphologies of the aggregates obtained from CH_3CN/H_2O (1:1) cast films. Fig. 2, panels *a* and *b* show TEM micrographs on films obtained from the polymer. In Fig. 3, panel *a* shows a TEM micrograph on a film obtained from a Fe^{III}-Cyt c solution, whilst panels *b* and *c* show TEM micrographs on a film obtained from a solution that contained both the polymer and Fe^{III}-Cyt c. A rationalization of

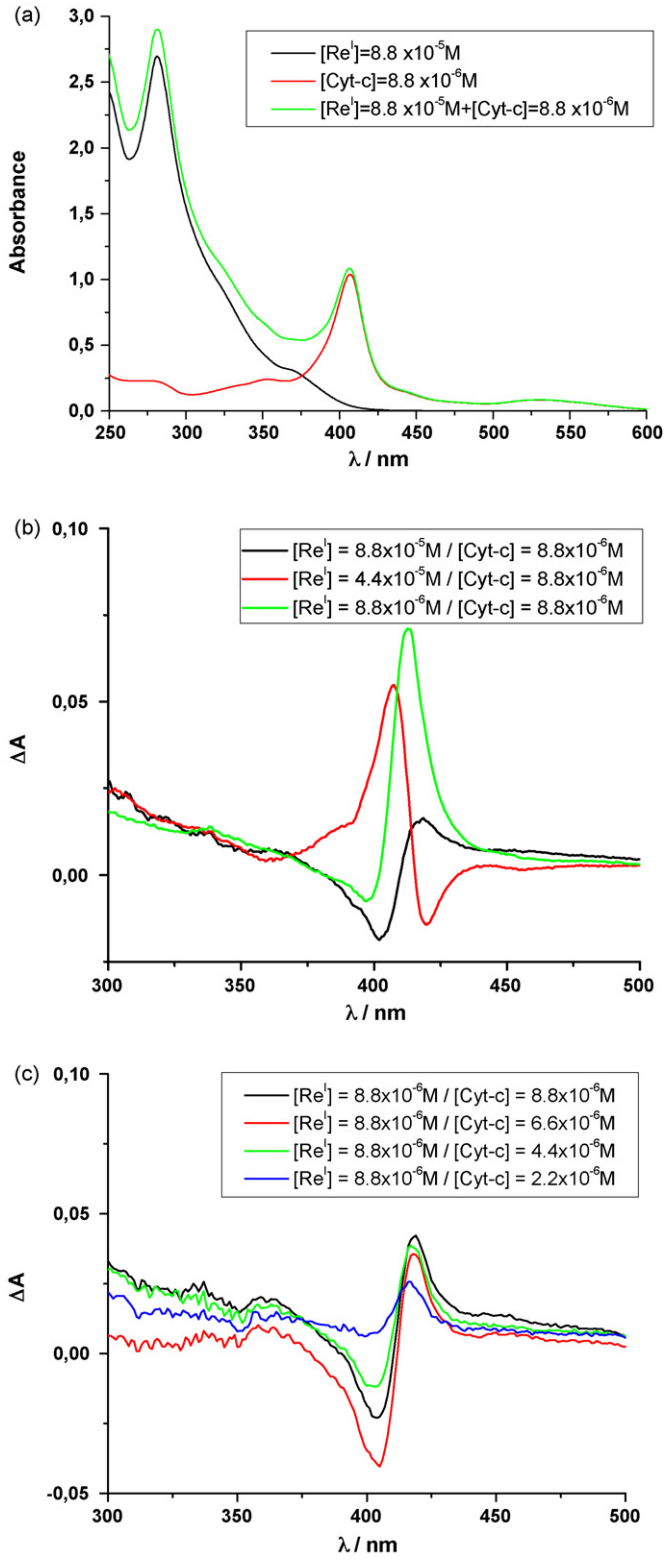

Fig. 1. (a) Absorption spectrum of a solution of ReP4VP ($[Re^I] = 8.8 \times 10^{-5}$ M, black line); Fe^{III}-Cyt c (8.8×10^{-6} M, red line) and a solution containing both together ReP4VP ($[Re^I] = 8.8 \times 10^{-5}$ M) and Cyt c (8.8×10^{-6} M) (green line). (b) Typical difference spectra recorded with solutions containing 8.8×10^{-6} M Fe^{III}-Cyt c and various concentrations of ReP4VP ($[Re^I]$ between 8.8×10^{-6} M and 8.8×10^{-5} M). (c) Difference spectra recorded with solutions containing ReP4VP ($[Re^I] = 8.8 \times 10^{-6}$ M) and various concentrations of Fe^{III}-Cyt c between 2.2×10^{-6} M and 8.8×10^{-6} M. See text for details. (For interpretation of the references to colour in this figure legend, the reader is referred to the web version of the article.)

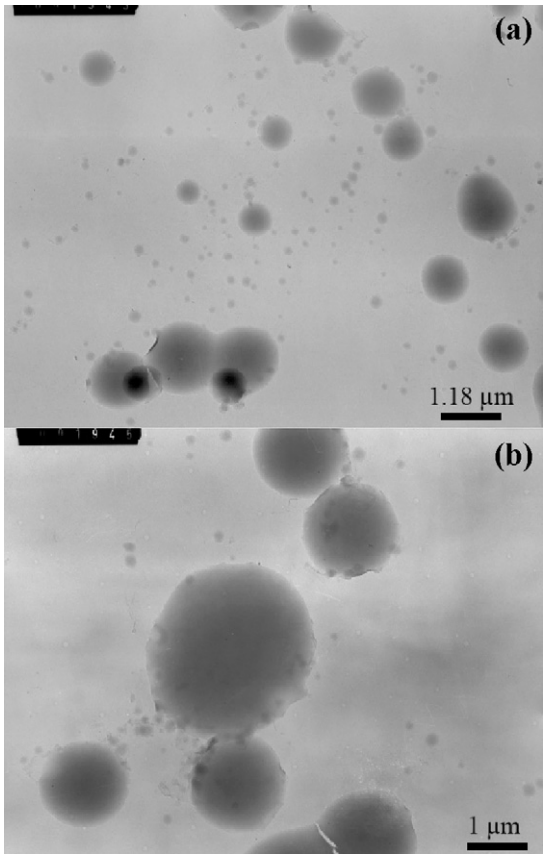

Fig. 2. TEM micrographs from CH_3CN/H_2O (1:1) cast films of polymer ReP4VP (panels a and b). The films were prepared from CH_3CN/H_2O (1:1) solutions with $[Re^I] = 2.6 \times 10^{-4}$ M. See text for details.

the shapes based on the aggregation of multiple strands of polymer is given in Section 4.

3.3. *Species formed by the photochemical and thermal reduction of ReP4VP*

Transient absorption spectra in the 15 ns to microsecond time domain were recorded with a 351 nm excimer laser flash photolysis set-up. The irradiation of the polymer produces transient spectra with the absorption bands of the $-Re^I(CO)_3(tmphen)^+$ MLCT excited state [22], which is shown in Fig. 4a. The reductive quenching of the MLCT excited state was investigated using the flash photolysis technique. Deaerated ReP4VP ($[Re^I] = 1.6 \times 10^{-4}$ M) solutions in CH_3CN containing triethylamine (TEA) as the excited state quencher were used for the studies. Transient spectra displaying two absorption bands with $\lambda_{max} = 420$ and 560 nm were recorded when two different TEA concentrations, namely [TEA] = 0.1 and 0.2 M, where used for the excited state quenching. Fig. 4b shows that the absorption bands at $\lambda_{max} = 420$ and 560 nm have nearly the same intensity when [TEA] = 0.1 M. However, the 420 nm band recorded with [TEA] = 0.2 M is more intense than the 560 nm band recorded with either TEA concentration. The transients generated in flash photolysis experiments with [TEA] = 0.1 M and 0.2 M decay in a few microseconds via a process that is kinetically of a first order in the concentration of the transient. The lifetime, $\tau = 6.3$ μs, is independent of the TEA concentration.

The spectra in Fig. 4b is attributed to the photogeneration of pendent $-Re^I(CO)_3(tmphen)^\bullet$ chromophores. To confirm this assignment, the same chromophores were generated by pulse radiolysis of ReP4VP ($[Re^I] = 5.3 \times 10^{-5}$ M) in MeOH deaerated with streams of N_2. The reaction between e^-_{solv} and ReP4VP was

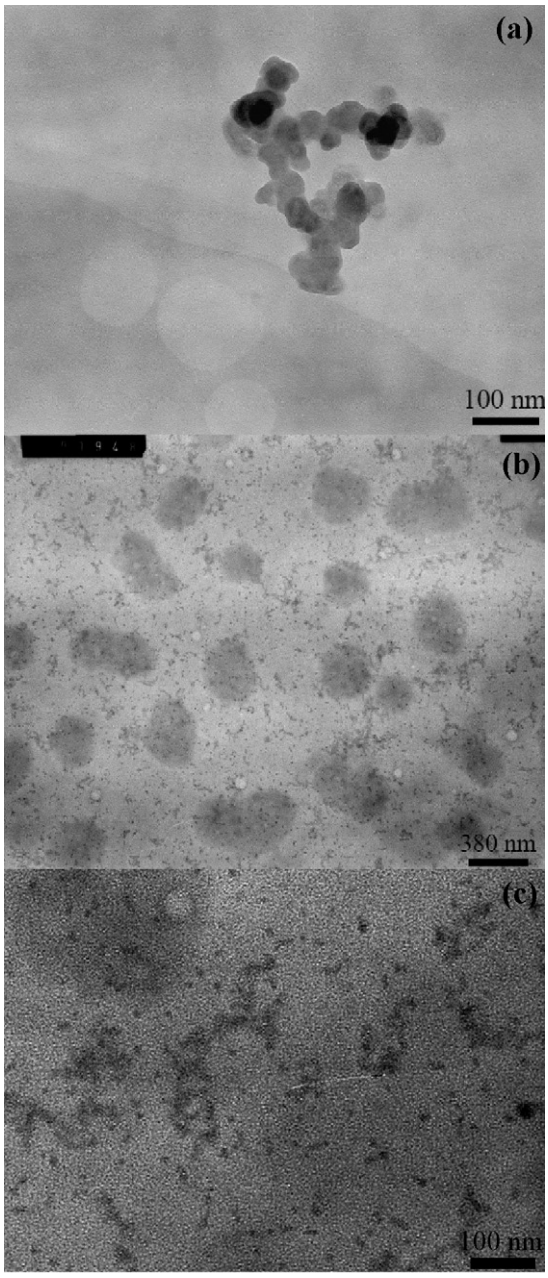

Fig. 3. TEM micrographs from CH_3CN/H_2O (1:1) cast films of Fe^{III}-Cyt c (panel a) and ReP4VP and Fe^{III}-Cyt c adducts (panels b and c). The films were prepared from CH_3CN/H_2O (1:1) solutions with $[Re^I] = 2.6 \times 10^{-4}$ M and $[Fe^{III}\text{-Cyt c}] = 2.6 \times 10^{-4}$ M, respectively. See text for details.

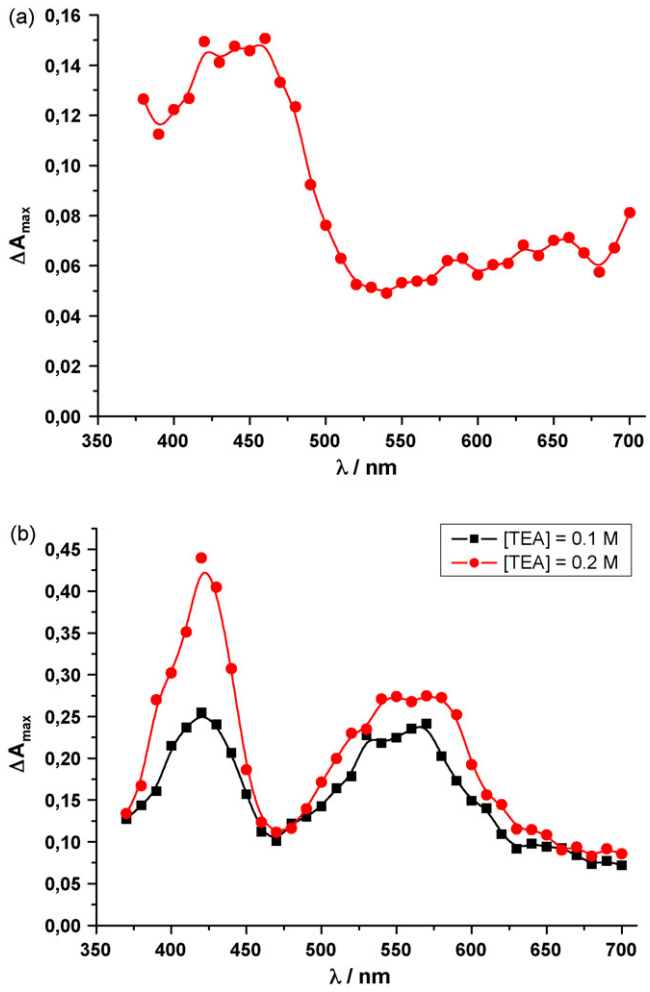

Fig. 4. (a) Transient spectra recorded in flash photolysis experiments of ReP4VP ($[Re^I] = 1.6 \times 10^{-4}$ M) in deaerated CH_3CN (b) Transient spectra recorded in flash photolysis experiments of ReP4VP ($[Re^I] = 1.6 \times 10^{-4}$ M) in deaerated CH_3CN containing TEA in concentrations 0.1 and 0.2 M. See text for details.

completed within the first μs after the radiolytic pulse with a rate constant $k = (2.1 \pm 0.2) \times 10^{10}\ M^{-1}\ s^{-1}$. The transient spectrum that is generated by the e^-_{solv} reaction, Fig. 5, exhibited two absorption bands with $\lambda_{max} = 420$ and 560 nm. It bears a strong resemblance with the spectrum photogenerated when the MLCT excited state reacts with 0.1 M TEA, Fig. 4b. After the reaction of the e^-_{solv} with the polymer was completed, the absorption bands at $\lambda_{max} = 420$ and 560 nm have nearly the same intensity. The transient spectrum shows a decrease of the $\lambda_{max} = 560$ nm band, relative to that at 420 nm, after a 3 ms delay from the radiolytic pulse. When solutions of ReP4VP were deaerated with streams of N_2O instead of N_2, all the radiolytically generated radicals were converted to $C^{\bullet}H_2OH$ radicals in less than 1 μs. The radiolytic pulse caused no changes in the spectrum of the solution. This experiment demonstrated that $C^{\bullet}H_2OH$ radicals do not reduce the tmphen ligand in ReP4VP and

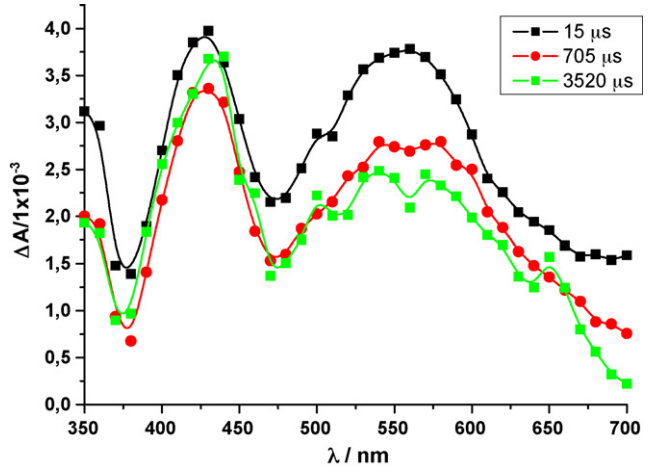

Fig. 5. Transient spectra recorded at several delay times after the radiolytic pulse in pulse radiolysis experiments of N_2-deaerated methanolic solutions of ReP4VP. See text for details.

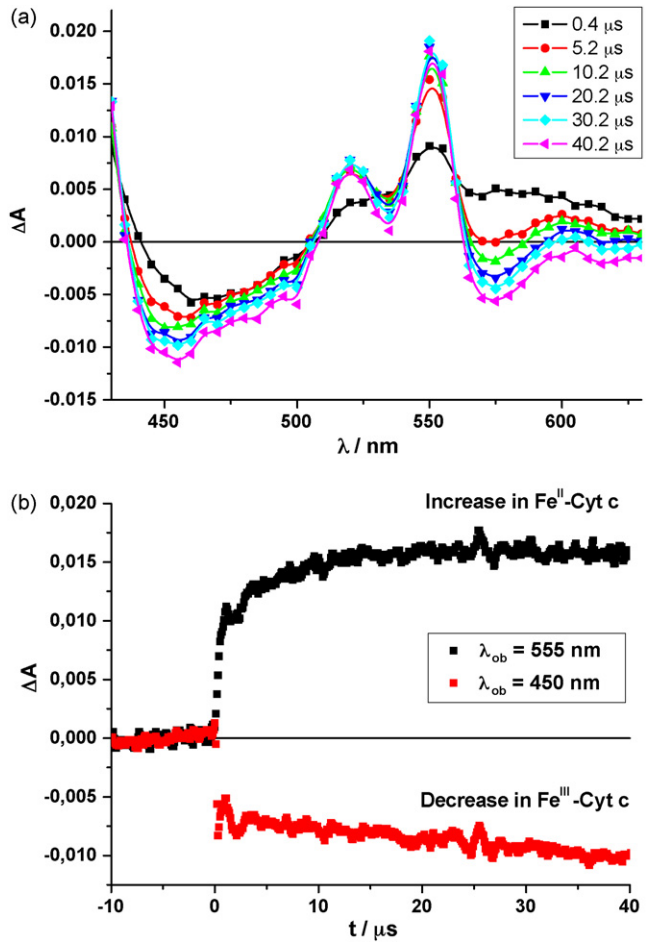

Fig. 6. (a) Transient spectra recorded at several delay times after the laser pulse in flash photolysis experiments (λ_{exc} = 351 nm) using CH_3CN/H_2O (1:1, v:v) deaerated solutions containing ReP4VP ([Re^I] = 1.1×10^{-4} M), TEA 0.06 M and Fe^{III}-Cyt c 5×10^{-5} M, respectively. (b) Oscillographic traces recorded at λ_{ob} = 555 and 450 nm in flash photolysis experiments of the system Re^I polymer/TEA/Cyt c/CH_3CN–H_2O(1:1). An increase of [Fe^{II}-Cyt c] is observed at λ_{ob} = 555 nm while a decrease of [Fe^{III}-Cyt c] is monitored at λ_{ob} = 455 nm. See text for details.

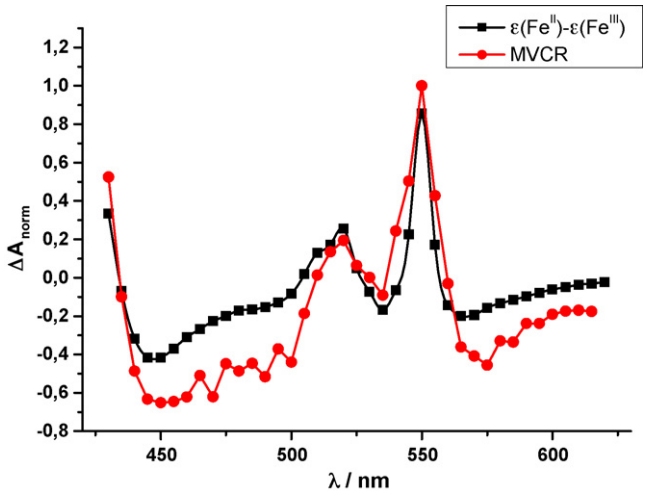

Fig. 7. Comparison of difference spectra between ferro- and ferricytochrome [$\varepsilon(Fe^{II})$–$\varepsilon(Fe^{III})$ taken from references [35] and [36]] and the difference spectra of the first contribution obtained using the MVCR technique. See text for details.

that the absorbance changes in Fig. 5 are caused by the reaction of e^-_{solv} with the Re^I pendants.

3.4. Photoinduced reduction of the adduct of Fe^{III}-Cyt c with ReP4VP

The reduction of Fe^{III}-Cyt c to Fe^{II}-Cyt c in the adduct was investigated using the 351 nm flash photolysis set-up. N_2-deaerated solutions containing ReP4VP ([Re^I] = 1.1×10^{-4} M), TEA 0.06 M and Fe^{III}-Cyt c 5×10^{-5} M in a 50% (v:v) CH_3CN–H_2O mixed solvent were used in these experiments. The photoinduced changes in the spectrum of the solution, Fig. 6a, show the increase of Fe^{II}-Cyt c with time after the flash irradiation. Oscillographic traces in Fig. 6b show that a fraction of Fe^{II}-Cyt c is formed, however, during the flash irradiation. To investigate if the irradiation of Fe^{III}-Cyt c could contribute to the optical transients in Fig. 6a, similar flash photochemical experiments were carried out with blanks containing only TEA and Fe^{III}-Cyt c. The flash irradiation of the solution produced no change in the absorption spectrum of the solution after the laser pulse showing that Fe^{III}-Cyt c was photoinert under these experimental conditions. Two processes may account for the prompt formation of Fe^{II}-Cyt c, Fig. 6. In one of them, the reduction of Fe^{III}-Cyt c to Fe^{II}-Cyt c is driven by the oxidative quenching of the Re^I pendants' MLCT excited state by Fe^{III}-Cyt c. In the other process, the formation of Fe^{II}-Cyt c results from a secondary process occurring after the reductive quenching of the excited states by TEA. The flash irradiation of a blank containing ReP4VP ([Re^I] = 1.1×10^{-4} M) and Fe^{III}-Cyt c 5×10^{-5} M in a 50% (v:v) CH_3CN–H_2O mixed solvent produces the transient spectrum of the Re^I pendants' MLCT excited state. No Fe^{II}-Cyt c is produced during the flash irradiation or as a consequence of the excited state decay. Moreover, the lifetimes of the MLCT excited state biexponential decay ($\tau_{fast} \sim 4.7 \times 10^2$ ns and τ_{slow} = 1.8 μs) are those expected for the unquenched excited state relaxation ($\tau_{fast} \sim 7.4 \times 10^2$ ns and τ_{slow} = 3.4 μs in neat CH_3CN) [22]. The decrease in τ_{fast} and τ_{slow} in CH_3CN–H_2O mixed solvent relative to their values in neat CH_3CN is in agreement with a decrease in the luminescence quantum yield (see below) in CH_3CN–H_2O mixed solvent relative to neat CH_3CN. A biexponential decay in transient absorbance of ReP4VP could be related to MLCT annihilation processes in addition to the first order decay due to the presence of excited chromophores in close proximity in the polymer [22]. It must be concluded, therefore, that Fe^{II}-Cyt c is formed from a secondary process occurring after the reductive quenching of the excited states by TEA.

The analysis of the time-resolved difference spectra, Fig. 6, was performed using MVCR techniques. Both Factor Analysis and Singular Value Decomposition were used for the estimation of the number of independent contributions yielding a value of n = 2. The results of self-modeling curve resolution obtained with the ALS algorithm are shown in Figs. 7 and 8. Fig. 7 shows the spectral contribution of the first factor in comparison with the difference spectra between Fe^{III}-Cyt c and Fe^{II}-Cyt c taken from the literature [35,36]. The spectral profile of the second factor is shown in Fig. 8 in comparison with the spectrum of $-Re^I(CO)_3(tmphen)^\bullet$ from pulse radiolysis and flash photolysis experiments in the presence of TEA. It is noteworthy that although there is not a perfect match between the spectral profile of the second factor and the spectrum attributable to $-Re^I(CO)_3(tmphen)^\bullet$ species, the position of the valley and maximum are coincident. According to the Singular Value Decomposition technique, the spectral contribution of the second factor is much smaller than that of the first factor in agreement with the highly different extinction coefficients of $-Re^I(CO)_3(tmphen)^\bullet$ and Fe^{III}-Cyt c (see below). Therefore, differences observed below 500 nm may be due to an incomplete splitting of the spectral contributions since both factors are highly coupled in this wavelength range.

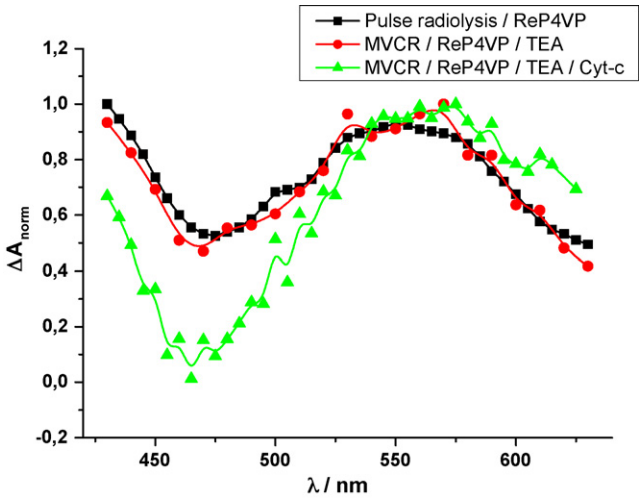

Fig. 8. Comparison of difference spectra between pulse radiolysis of N_2-deaerated methanolic solutions of ReP4VP and difference spectra of the second contribution obtained using the MVCR technique. See text for details.

4. Discussion

Fe^{III}-Cyt c is highly ionized with a net positive charge of +9 in the oxidized state at physiological pH. The positively charged residues are homogeneously distributed on the protein surface. On the other hand, the distribution of the negative surface charges is asymmetric, with nearly all the negatively charged residues located in the small area on the back surface of Fe^{III}-Cyt c [1]. Therefore, an asymmetric charge distribution in horse Fe^{III}-Cyt c results in an electric dipole moment of ~300 D [2]. This dipole moment is created by the absence of negative charges near the solvent-accessible heme edge [3]. The heme is covalently attached to Cys14 and Cys17, and the porphyrin plane, which is nearly perpendicular to the protein surface, stands in a crevice surrounded by the polypeptide chain of aminoacids [1]. This region of the protein surface is surrounded by positively charged lysines [1]. From recent crystallographic studies on the 3D structure of Fe^{III}-Cyt c (PDB 1HRC) [37] it is known that in heart Fe^{III}-Cyt c the iron atom lies in the plane of the porphyrin ring with its fifth coordination site occupied by a nitrogen atom of the imidazole ring of histidine-18 and its remaining coordination site by the sulfur atom of methionine-80. Iron-binding ligands such as azide, cyanide and imidazole can coordinate to the iron, and the evidence suggests that these ligands bind by displacing the methionine-80 [38,39,40]. The methionine-80 sulfur atom displacement is evidenced by a decrease in the 695 nm absorbance of the protein [40].

4.1. Formation of adducts

Adducts formed between ReP4VP and Fe^{III}-Cyt c are revealed by those changes in the absorption spectrum that are shown in Fig. 1b, c. This association probably involves hydrogen bonds between the positively charged lysine groups in Fe^{III}-Cyt c and the nitrogen atom of the free pyridines in ReP4VP. A similar adduct-stabilizing hydrogen bonding between poly(4-vinylpyridine) and Fe^{III}-Cyt c has been previously postulated [1].

Binding studies between Fe^{III}-Cyt c and ReP4VP, Fig. 1a, b, were performed in a 20% (v:v) CH_3CN in H_2O mixed solvent. Addition of 20% of CH_3CN to aqueous Fe^{III}-Cyt c solutions was needed in order to dissolve ReP4VP. Lower percentages of CH_3CN, i.e., 10%, did not dissolve the polymer. The Fe^{III}-Cyt c is denatured in mixed solvents with 20% of CH_3CN even in the absence of ReP4VP. The unfolding and denaturing of Fe^{III}-Cyt c has been previously observed after addition of methanol to aqueous solutions of the protein [41]. An absorption feature in the spectrum of Fe^{III}-Cyt c at 695 nm disappears as a consequence of denaturation. Such a change in the spectrum of Fe^{III}-Cyt c precluded us from using the 695 nm absorbance change to follow the coordination of Fe^{III}-Cyt c to ReP4VP. Nevertheless, the coordination of the free pyridines of ReP4VP to the iron center cannot be ruled out. On this basis, the spectral changes shown in Fig. 1b and c are accounted for either the coordination of the pendant pyridines to Fe^{III}-Cyt c or the formation of hydrogen bonds between the protein and the Re^{I} polymer, or both.

Morphologies of the compounds shown in Figs. 2 and 3 were obtained from cast films prepared in the acetonitrile-water mixed solvent. Panels a and b of Fig. 2 show that in solid phase, the Re^{I} pendants of ReP4VP aggregate and form isolated nanodomains that are dispersed in the poly-4-vinylpyridine backbone. The sizes of the nanodomains are very polydisperse with outer diameters ranging from 140 nm to large compound nanodomains with diameters up to 2.8 μm. Since strands of ReP4VP with an average length of ~ 200 nm cannot be coiled into these big structures, the observed nanodomains must correspond to an aggregate of many strands. Panel a of Fig. 3 shows aggregates formed by Fe^{III}-Cyt c. It can be observed that spherical aggregates about 30–50 nm in diameter are crowded together into branched short rods. In the heme-free apo Cyt c, which also has a disordered structure in solution, the formation of aggregates upon varying the pH was put in evidence by AFM and dynamic light scattering techniques [4c]. It should be noted that the dimensions of these nanodomains shown in Fig. 3 are considerably larger than the diameter of Fe^{III}-Cyt c, which is about 4 nm. As a result, it is likely that they contain several molecules of the protein. Panel b shows that the morphology of the adduct between the Re^{I} polymer and Fe^{III}-Cyt c is quite different than that of the Re^{I} polymer alone. In the cast films obtained from solutions containing ReP4VP and Fe^{III}-Cyt c, large compound nanodomains have disappeared and distorted spherical nanodomains about 300 nm in diameter remain. This change in size, from the nanodomains in Fig. 2a, b to the nanodomains in Fig. 3b, suggests that the number of strands forming the nanodomains of ReP4VP is reduced by the association of the polymer with Fe^{III}-Cyt c. It must also be noted in Fig. 3c that aggregates formed by Fe^{III}-Cyt c can still be observed in addition to the ReP4VP polymer aggregates. Aggregation and adduct formation can be rationalized with the aid of eqs. (4)–(6)

$$m\{[(vpy)_2vpyRe^{I}(CO)_3(tmphen)^+]\}_{n\sim200} \xrightarrow{CH_3CN/H_2O} \langle\{[(vpy)_2vpyRe^{I}(CO)_3(tmphen)^+]\}_{n\sim200}\rangle_m \quad (4)$$

$$\underset{\text{Native protein}}{N\,Fe^{III}-Cyt\,c} \xrightarrow{CH_3CN/H_2O} \underset{\text{denaturation and aggregation}}{(Fe^{III}-Cyt\,c)_N} \quad (5)$$

$$\langle\{[(vpy)_2vpyRe^{I}(CO)_3(tmphen)^+]\}_{n\sim200}\rangle_m + (Fe^{III}-Cyt\,c)_n \rightarrow \text{Adducts} \quad (6)$$

The polydispersity of the ReP4VP nanoaggregates is very high with outer diameters varying from 140 nm to ~3 μm. The formation of different adducts between the ReP4VP and Fe^{III}-Cyt c reduces the sizes of the ReP4VP nanoaggregates to distorted spheres of about 300 nm. The adducts may contain discrete Fe^{III}-Cyt c units as well as aggregates $(Fe^{III}$-Cyt $c)_N$ interacting with a ReP4VP polymer strand. Therefore, TEM experiments reinforce the UV–vis results about adduct formation between both species. Adduct formation is a necessary condition for electron transfer to occur between $-Re^{I}(CO)_3(tmphen)^{\bullet}$ pendants and Fe^{III} heme. If both species were far apart (for instance in the case where the polymer ReP4VP and

Fe^{III}-Cyt c were not interacting between them), electron transfer would be impossible.

4.2. Ground-state redox reactions

The spectrum of the transient recorded just after the reaction of e^-_{solv} and ReP4VP (at 15 μs in Fig. 5) can be associated with the $-Re^I(CO)_3(tmphen)^\bullet$ species in the ReP4VP. Since a concentration $[e^-_{solv}] \sim 2\times10^{-6}$ M of e^-_{solv} is generated in the pulse radiolysis experiments, only a small percentage (~4%) of the total number of $-Re^I(CO)_3(tmphen)^+$ chromophores is reduced to $-Re^I(CO)_3(tmphen)^\bullet$ by the solvated electrons. Changes of the absorption spectrum in the millisecond time domain, e.g., at 3.5 ms in Fig. 5, must be ascribed to the demise of the $-Re^I(CO)_3(tmphen)^\bullet$ radicals. The demise of the radicals must occur by a slower disproportionation reaction that possibly demands larger diffusive displacements of polymer strands.

4.3. Excited-state redox processes of the polymer pendants in the absence of Fe^{III}-Cyt c

Reduction of the polymer excited states was effected in less than 25 ns by TEA. A growth of the $-Re^I(CO)_3(tmphen)^\bullet$ spectrum that showed an additional reduction of $-Re^I(CO)_3(tmphen)^+$ groups by reducing radicals derived from TEA oxidation in the polymer was not observed. The prompt growth of the $-Re^I(CO)_3(tmphen)^\bullet$ spectrum was followed by a rapid ($\tau = 6.2$ μs) decay of the spectrum with a first-order kinetics. The shape of the spectrum recorded with [TEA] = 0.1 M in Fig. 4 is very similar to that in Fig. 5, which is associated with the initial reduction product $-Re^I(CO)_3(tmphen)^\bullet$. After comparison of the ΔA_{max} of Figs. 4b and 5, it is estimated that the concentration of $-Re^I(CO)_3(tmphen)^\bullet$ produced in flash photolysis experiments is at least two orders of magnitude higher than the one generated in pulse radiolysis experiments, i.e., $[-Re^I(CO)_3(tmphen)^\bullet] \sim 1\times10^{-4}$ M in the flash photolysis experiment. This estimation is only a rough one for $[-Re^I(CO)_3(tmphen)^\bullet]$ since it is assumed that the extinction coefficient of $-Re^I(CO)_3(tmphen)^\bullet$ has the same value either in CH_3CN or MeOH. The shape of the spectrum recorded with [TEA] = 0.2 M in Fig. 4 resembles that at longer times in pulse radiolysis experiments. However, both transients decay with the same kinetic behavior. A disproportionation reaction of $-Re(CO)_3(tmphen)^\bullet$ radicals, Eqs. (7) and (8), may occur sequentially [10,23–25]

$$-Re^I(CO)_3(tmphen)^\bullet + TEAH^+ \rightarrow Re^I(CO)_3(tmphenH)^{\bullet+} + TEA \quad (7)$$

$$2\ -Re^I(CO)_3(tmphenH)^{\bullet+} \rightarrow Re^I(CO)_3(tmphenH_2)^+ + Re^I(CO)_3(tmphen)^+ \quad (8)$$

Equations (7) and (8) represent the protonation of $-Re^I(CO)_3(tmphen)^\bullet$ by available $TEAH^+$ in the polymer and the slow diffusive motion of the polymeric strands that allows a bimolecular encounter of $-Re^I(CO)_3(tmphenH)^{\bullet+}$ pendants, respectively. $TEAH^+$ species are produced by deprotonation of the radical cation $(CH_3CH_2)_3N^{\bullet+}$, Eq. (9).

$$(CH_3CH_2)_3N^{\bullet+} + TEA \rightarrow (CH_3CH_2)_2N(^\bullet CHCH_3) + TEAH^+ \quad (9)$$

The whole process occurs in the millisecond–second time domain in pulse radiolysis experiments where the $-Re^I(CO)_3(tmphen)^\bullet$ radical species are produced in low concentrations (~2×10^{-6} M). Because the radicals will be separated from each other by large distances, diffusive motions of the polymer strands are required to bring them together. In flash photolysis experiments, however, the initial concentration of $-Re^I(CO)_3(tmphen)^\bullet$ radical species generated by reductive quenching of the excited states by TEA is very high (between 80% and 90% of the total number of $-Re^I(CO)_3(tmphen)^+$ pendants) and diffusive motions are hardly required. In this condition, the disproportionation occurs much faster, i.e., in the microsecond time domain. In addition, similarities between the spectra generated in flash photolysis and pulse radiolysis experiments suggest that at low TEA concentration the predominant decay species is $-Re^I(CO)_3(tmphen)^\bullet$. At the higher TEA concentration, Eqs. (7) and (9) become very fast and the protonated $Re^I(CO)_3(tmphenH)^{\bullet+}$ is the predominant transient species.

4.4. Excited-state redox reactions in the ReP4VP–Fe^{III}-Cyt c adduct

As can be observed from Fig. 6, the photoinduced reduction of Fe^{III}-Cyt c to Fe^{II}-Cyt c occurs within a 40 μs time scale by a two-step process. Initially, there is a prompt increase of the 555 nm absorbance (characteristic of Fe^{II}-Cyt c) mirrored by a prompt decrease in the 450 nm absorbance (characteristic of Fe^{III}-Cyt c). This fast reduction occurs nearly within the laser lifetime. A subsequent slower reduction occurs within a 1–40 μs time scale. The analysis of the normalized concentration profiles obtained for the first factor with the MVCR technique shows that the slower process kinetically is a first-order process with a lifetime of $\tau = (15 \pm 1)$ μs. The fast reduction process contributes with nearly 50% of the total amount of Fe^{II}-Cyt c generated in the photoinduced reduction. Eqs. (10) and (11) account for the formation of MLCT excited states in a polymer strand and subsequent quenching by TEA

$$[(vpy)_2\text{-}vpyRe^I(CO)_3(tmphen)^+]_{n\sim200} + h\nu \rightarrow [(vpy)_2\text{-}vpyRe^I(CO)_3(tmphen)^{+*}]_p[(vpy)_2\text{-}vpyRe^I(CO)_3(tmphen)^+]_q \quad (10)$$

$$[(vpy)_2\text{-}vpyRe^I(CO)_3(tmphen)^{+*}]_p \times [(vpy)_2\text{-}vpyRe^I(CO)_3(tmphen)^+]_q + pTEA \rightarrow [(vpy)_2\text{-}vpyRe^I(CO)_3(tmphen)^\bullet]_p \times [(vpy)_2\text{-}vpyRe^I(CO)_3(tmphen)^+]_q + pTEA^{\bullet+} \quad (11)$$

In Eq. (10), $-Re^I(CO)_3(tmphen)^{+*}$ denotes the MLCT excited state of the $-Re^I(CO)_3(tmphen)^+$ chromophore. In CH_3CN/H_2O solvent mixture, the reduction of MLCT excited states in ReP4VP produces $-Re^I(CO)_3(tmphen)^\bullet$ radicals in concentrations $[-Re^I(CO)_3(tmphen)^\bullet]_0 \sim 2\times10^{-6}$ M, eq. (11). Some of those $-Re^I(CO)_3(tmphen)^\bullet$ radicals that may be close in space to bound Fe^{III}-Cyt c in the adduct may participate in the fast Fe^{III}-Cyt c reduction evidenced by the prompt absorbance changes in Fig. 6. Based on the results of MVCR analysis presented in Figs. 7 and 8, the time-resolved spectra in Fig. 6 must be interpreted as the changes in the solution spectrum when $-Re^I(CO)_3(tmphen)^\bullet$ pendants decay and Fe^{II}-Cyt c is formed. It is noteworthy that as the difference between the molar extinction coefficients of Fe^{II}-Cyt c and Fe^{III}-Cyt c, i.e., $\Delta\varepsilon(Fe^{II}\text{–}Fe^{III})$, is one order of magnitude higher than the molar extinction coefficient of $-Re^I(CO)_3(tmphen)^\bullet$, the contribution of the radical $-Re^I(CO)_3(tmphen)^\bullet$ to the absorption features of Fig. 6 is only relevant at wavelengths between 600 and 700 nm, where $\Delta\varepsilon(Fe^{II}\text{–}Fe^{III})$ is small. From the MVCR analysis we also obtained an estimation of the concentrations generated in flash photolysis experiments. The initial concentration of $-Re^I(CO)_3(tmphen)^\bullet$ ($[-Re^I(CO)_3(tmphen)^\bullet]_0$) is ~$2\times10^{-6}$ M. The maximum conversion from Fe^{III}-Cyt c to Fe^{II}-Cyt c yields $[Fe^{II}\text{-Cyt}]_{max} \sim 5\times10^{-6}$ M.

The initial concentration of $-Re^I(CO)_3(tmphen)^\bullet$ ($[-Re^I(CO)_3(tmphen)^\bullet]_0$) produced in flash photolysis of solu-

tions containing ReP4VP, TEA and Fe^{III}-Cyt c in a 1:1 (v:v) CH_3CN–H_2O mixed solvent is two orders of magnitude lower than the concentration generated in neat CH_3CN. This difference is explained on the basis of two solvent effects: (i) the emission quantum yield of ReP4VP is nearly three times lower in a 50% (v:v) CH_3CN in H_2O mixed solvent than in neat CH_3CN; (ii) TEA concentration decreases in a 50% (v:v) CH_3CN in H_2O mixed solvent due to protonation.

Because the radicals produced by the photoinduced TEA oxidation, Eq. (11), do not react with ReP4VP, the demise of the $TEA^{\bullet}$ radicals occurs via Eqs. (12) and (13) in competition with the slow reduction of Fe^{III}-Cyt c [42,43].

$$TEA^{\bullet+} + TEA \rightarrow TEA^{\bullet} + TEAH^{+} \quad (12)$$

$$2\,TEA^{\bullet} \rightarrow TEA + (CH_3CH_2)_2N - CH = CH_2 \quad (13)$$

while Eq. (13) has already been discussed in the literature [42,43], changes in the spectrum shown in Fig. 6 document the reaction of the TEA radicals with the Fe^{III}-Cyt c adduct.

5. Conclusions

Interest in nonnative and denatured states of proteins has increased in the last years since these less ordered states play important roles in biological processes such as protein folding and stability. Therefore, electron-transfer studies carried out with denatured proteins may be relevant to unravel unanswered questions in biological phenomena. Fe^{III}-Cyt c is denatured in CH_3CN/water mixtures and tends to form aggregates. These aggregates interact with a Re^{I} polymer, i.e., ReP4VP, by the formation of adducts as revealed by UV–vis and TEM spectroscopy. The reduction of the $-Re^{I}(CO)_3(tmphen)^{+}$ chromophores in a polymer strand, achieved by the reductive quenching of the MLCT excited state by TEA and/or by the reaction between e^{-}_{solv} and the Re^{I} chromophore in pulse radiolysis experiments, produces $-Re^{I}(CO)_3(tmphen)^{\bullet}$ and $-Re^{I}(CO)_3(tmphenH)^{\bullet+}$ as the main species. When the reductive quenching of the polymer luminescence was carried out in the presence of Fe^{III}-Cyt c, a rapid electron transfer ($\tau < 20$ ns) occurred from the $-Re^{I}(CO)_3(tmphen)^{\bullet}$ to the Fe^{III} center in the heme to produce Fe^{II}-Cyt c. This fast reduction process contributes nearly half of the total amount of Fe^{II}-Cyt c generated in the photoinduced reduction. A slower reduction process ascribed to the reaction of Fe^{III}-Cyt c with $TEA^{\bullet}$ radicals, with a lifetime of $\tau = 15$ μs, occurs in competition with the demise of these radicals to form TEA and $(CH_3CH_2)_2N$–CH═CH_2.

Acknowledgments

Work supported in part by ANPCyT Grant No. PICT 26195, CONICET-PIP 6301/05, Universidad Nacional de La Plata, and CICPBA. G. F. acknowledges support from the Office of Basic Energy Sciences of the U.S. Department of Energy. L.L.B.B. acknowledges support from CONICET. F.G.E and E.W. are members of CONICET. This is contribution No. NDRL – 4789 from the Notre Dame Radiation Laboratory.

References

[1] X. Qu, T. Lu, S. Dong, J. Mol. Cat. A: Chem. 102 (1995) 111–116.
[2] W.H. Koppenol, J.D. Rush, J.D. Mills, E. Margoliash, Mol. Biol. Evol. 8 (1991) 545–558.
[3] W.H. Koppenol, E. Margoliash, J. Biol. Chem. 257 (1982) 4426–4437.
[4] (a) E. Margoliash, Proc. Natl. Acad. Sci. (USA) 50 (1963) 672–679;
(b) K. Chattopadhyay, S. Mazumdar, Biochemistry 42 (2003) 14606–14613;
(c) L. Liang, P. Yao, M. Jiang, G. Zhang, Y. Yan, Langmuir 21 (2005) 10662–10670;
(d) K.A. Dill, D. Shortle, Annu. Rev. Biochem. 60 (1991) 795–825;
(e) D. Shortle, FASEB J. 10 (1996) 27–34.
[5] (a) R.Q. Liu, L. Geren, P. Anderson, J.L. Fairris, N. Peffer, A. McKee, B. Durham, F. Millett, Biochimie 77 (1995) 549–561;
(b) D.H. Murgida, P. Hildebrandt, Chem. Soc. Rev. 37 (2008) 937–945.
[6] B. Durham, L.P. Pan, J.E. Long, F. Millett, Biochemistry 28 (1989) 8659–8665.
[7] I-Jy Chang, H.B. Gray, J.R. Winkler, J. Am. Chem. Soc. 113 (1991) 7056–7057.
[8] L.P. Pan, B. Durham, J. Wolinska, F. Millett, Biochemistry 27 (1988) 7180–7184.
[9] (a) C. Kutal, M.A. Weber, G. Ferraudi, D. Geiger, Organometallics 4 (1985) 2161–2166;
(b) J. Hawecker, J.-M. Lehn, R. Ziessel, J. Chem. Soc., Chem. Commun. (1984) 328–330.
[10] E. Wolcan, G. Ferraudi, J. Phys. Chem. A 104 (2000) 9281–9286, references therein.
[11] W.E. Jones, L. Hermans Jr., B. Jiang, in: V. Ramamurthy, K.S. Schanze (Eds.), Multimetallic and Macromolecular Inorganic Photochemistry, vol. 4, Marcel Deker Inc., New York, 1999, chapter 1.
[12] M.Y. Ogawa, in: V. Ramamurthy, K.S. Schanze (Eds.), Multimetallic and Macromolecular Inorganic Photochemistry, vol. 4, Marcel Deker Inc, New York, 1999, chapter 3.
[13] D.J. Stufkens, A. Vlček Jr., Coord. Chem. Rev. 177 (1998) 127–179, references therein.
[14] G.D. Smith, K.A. Maxwell, J.M. DeSimone, T.J. Meyer, R.A. Palmer, Inorg. Chem. 39 (2000) 893–898.
[15] J.D. Petersen, in: V. Balzani (Ed.), Supramolecular Photochemistry, Reidel, Dordrecht, The Netherlands, 1987, p. 135.
[16] V. Balzani, F. Scandola, Supramolecular Photochemistry, Ellis Harwood, Chichester, UK, 1991, p. 355.
[17] M. Kaneko, E. Tsuchida, J. Polym. Sci. Macromol. Rev. 16 (1981) 397–522.
[18] E. Wolcan, M.R. Féliz, Photochem. Photobiol. Sci 2 (2003) 412–417.
[19] E. Wolcan, G. Ferraudi, M.R. Féliz, R.V. Gomez, L. Mickelsons, Supramol. Chem. 15 (2003) 143–148.
[20] M.R. Féliz, G. Ferraudi, Inorg. Chem. 43 (2004) 1551–1557.
[21] E. Wolcan, J.L. Alessandrini, M.R. Feliz, J. Phys. Chem. B 109 (2005) 22890–22898.
[22] L.L.B. Bracco, M.P. Juliarena, G.T. Ruiz, M.R. Féliz, G.J. Ferraudi, E. Wolcan, J. Phys. Chem. B 112 (2008) 11506–11516.
[23] M.R. Féliz, G. Ferraudi, J. Phys. Chem. 96 (1992) 3059–3062.
[24] M.R. Féliz, G. Ferraudi, H. Altmiller, J. Phys. Chem. 96 (1992) 257–264.
[25] J. Guerrero, O.E. Piro, E. Wolcan, M.R. Féliz, G. Ferraudi, S.A. Moya, Organometallics 20 (2001) 2842–2853.
[26] G.L. Hug, Y. Wang, C. Schöneich, P.-Y. Jiang, R.W. Fessenden, Radiat. Phys. Chem. 54 (1999) 559–566.
[27] G.V. Buxton, C.L. Greenstock, W.P. Helman, A.B. Ross, J. Phys. Chem. Ref. Data 17 (1988) 513–886.
[28] M.R. Féliz, G. Ferraudi, Inorg. Chem. 37 (1998) 2806–2810.
[29] N. Getoff, A. Ritter, F. Schwörer, P. Bayer, Radiat. Phys. Chem. 41 (1993) 797–801.
[30] L.M. Dorfman, in: R.F. Gould (Ed.), The Solvated Electron in Organic Liquids; Advances in Chemistry Series 50, American Chemical Society, Washington, DC, 1965, pp. 36–44.
[31] M. Simic, P. Neta, E. Hayon, J. Phys. Chem. 73 (1969) 3794–3800.
[32] (a) García Einschlag, F., 2005. Kinesim 9.5: Obra de software. Dirección Nacional del Derecho de Autor, Argentina. Expediente No. 395814;
(b) C. Ruckebusch, S. Aloise, L. Blanchet, J.P. Huvenne, G. Buntinx, Chemometr. Intell. Lab. Syst. 91 (2008) 17–27;
(c) M. Garrido, M.S. Larrechi, F.X. Rius, R. Tauler, Chemometr. Intell. Lab. Syst. 76 (2005) 111–120.
[33] M. Garrido, I. Lázaro, M.S. Larrechi, F.X. Rius, Anal. Chim. Acta 515 (2004) 65–73.
[34] (a) M. Blanco, A.C. Peinado, J. Mas, Anal. Chim. Acta 544 (2005) 199–205;
(b) M. Meloun, J. Čapek, P. Mikšik, R.G. Brereton, Anal. Chim. Acta 423 (2000) 51–68;
(c) P. Gemperline, E. Cash, Anal. Chem. 75 (2003) 4236–4243.
[35] W.D. Butt, D. Keilin, Proc. R. Soc. Lond. B 156 (1962) 429–458.
[36] J. Butler, G.G. Jayson, A.J. Swallow, Biochim. Biophys. Acta 408 (1975) 215–222.
[37] G.W. Bushnell, G.V. Louie, G.D. Brayer, J. Mol. Biol. 214 (1990) 585–595.
[38] N. Sutin, J.K. Kandell, J. Biol. Chem. 247 (1972) 6932–6936.
[39] P. George, S.C. Glauser, A. Schejter, J. Biol. Chem. 242 (1967) 1690–1695.
[40] A. Schejter, I. Aviram, Biochemistry 8 (1969) 149–153.
[41] H.R. Drew, R.E. Dickerson, J. Biol. Chem. 253 (1978) 8420–8427.
[42] M. Goez, I. Sartorius, J. Am. Chem. Soc. 115 (1993) 11123–11133.
[43] M. Goez, I. Sartorius, J. Phys. Chem. A 107 (2003) 8539–8546.